An Advanced Numerical Model of Gear Tooth Loading from Backlash and Profile Errors

Andrew Sommer, Jim Meagher, Xi Wu

ABSTRACT

This study demonstrates the early transient dynamic loading on teeth within a fixed-axis gear transmission arising from backlash and geometric manufacturing errors by utilizing a non-linear multi-body dynamics software model. Selection of the non-linear contact parameters such as the stiffness, force exponent, damping, and friction coefficients are presented for a practical transmission. Backlash between gear teeth which is essential to provide better lubrication on tooth surfaces and to eliminate interference is included as a defect and a necessary part of transmission design. Torsional vibration is shown to cause teeth separation and double-sided impacts in unloaded and lightly loaded gearing drives. Vibration and impact force distinctions between backlash and combinations of transmission errors are demonstrated under different initial velocities and load conditions. Additionally, the loading dynamics of a crank-slider mechanism with two-stage gear driving train is analyzed. The backlash and manufacturing errors in the first stage of the gear train are distinct from those of the second stage. By analyzing the signal at a location between the two stages, the mutually affected impact forces are observed from different gear pairs, a phenomenon not observed from single pair of gears.

1. Introduction

Gear trains with different designs play very important roles in automobiles, helicopters, wind turbines, and other modern industries. Excessive loading on the gear teeth may arise due to the combination of gear backlash and teeth defects. Without vibration health monitoring to ensure proper operation performance will degrade.

Dubowsky and Freudenstein [1, 2] developed a theoretical model to investigate the dynamic response of a mechanical system with clearance. Based on this research, Azar and Crossley [3] explored the dynamic behaviors of the engaged gearing systems with gear backlash, time-varying stiffness and damping of the gear teeth. Compared with above investigations, Yang and Sun [4] developed a more realistic dynamic model for a spur gear system with backlash. By taking the involute tooth profile into consideration, they were able to account for material compliance, energy dissipation, time-varying mesh stiffness and damping due to the contact teeth-pair alternating between one and two during the gear engagement. In order to accurately simulate the gear dynamic behavior, the gear mesh stiffness between meshing gear pairs should include at least two factors: local Hertzian deformation and tooth bending. Even though the authors only considered the Hertzian contact stiffness, the dynamic simulations for free vibration, constant load operation and sinusoidal excitation presented insightful results.

Two notable review papers that discuss the numerical modeling of gear dynamics are by Özgüven and Houser in 1988 [5] and by Parey and Tandon in 2003 [6]. Özgüven categorized the models as dynamic factor models, models with tooth compliance, models for gear dynamics, those for rotor dynamics, and those for torsional vibration. The listed goals for the studies included reliability, life, stress, loading, noise, and vibratory motion. Curiously, condition monitoring was not included. Early work modeled the meshing stiffness as either an average or piecewise linear variation. Parey and Tandon's review concentrated mostly on the modeling of defects but includes an extensive compilation of various lumped parameter models. Dalpiaz etc. [7] investigated a gear pair with a fatigue crack and discussed the effectiveness and sensitivity of the time-synchronous average (TSA) analysis, cyclostationary analysis, and traditional cepstrum analysis on the basis of experiment. Parey etc. [8] developed a six DOF nonlinear model for a pair of spur gears on two shafts, calculated the Hertzian stiffness for the tooth surface contact, and implemented the empirical mode decomposition (EMD) method to simulate the different defect widths. Many authors [9, 10, 11, 12] utilized different methods of estimating time-varying stiffness in order to get practical dynamic simulation results. Meagher and Wu etc. [13] presented three different dynamic system modeling strategies currently being used by researchers to identify diagnostic indicators of gear health: a strength of materials based lumped parameter model, non-linear quasi-static finite element modeling, and rigid multi-body kinematic modeling with

nonlinear contact stiffness. This research contrasts these methods of modeling gear dynamics by comparing their predicted stiffness cycle and its effect on dynamic response. Data from experiments are shown for the high contact ratio pair.

Previous research shows that the signal patterns due to the combination of backlash, time-varying gear mesh stiffness, and the involute profile errors, are very complicated and highly depend on gear train design and configurations. In other words, the signals from a specific gearing system are difficult to interpret until a series of modeling, testing and data processing work are carried out. However, it is not realistic to experimentally test each type of gear train for the specific fault patterns. To solve this issue, a virtual experiment method based on multi-body dynamics and nonlinear contact mechanics simulation is presented. Ebrahimi and Eberhard [14] used multi-body dynamics software to model gear mesh stiffness using a rigid-elastic model. Hertzian contact at the gear interface is used to represent gear elasticity as a compromise over fully elastic models; thereby reducing computational effort. Kong and Meagher etc. [15] modeled a large industrial gearbox used in a 12 m^3 electric mining shovel. The nonlinear contact mechanics is analyzed to predict the bearing support force variation and gear tooth loading of ideal gears and gears with defects using multi-body dynamics software. No gear backlash was considered. In this study, the authors demonstrate the importance of accurate geometric modeling of gear tooth involutes, and realistic center distance separation on the transient response of ideal and defective gears. The highly nonlinear character of loading and geometry requires special attention to Hertzian contact modeling. Once modeled accurately, double sided tooth impacts and associated loading can be determined as well as superposition of effects at a shaft intermediate to sets of gears.

2. One-stage Gear Train and Discussions

2.1. Multi-body kinematic model of a One-stage Gear Train

A rigid-elastic model [17] of a pair of meshing gears is shown in Fig.1. Fig.2 shows the eccentric pinion tooth with chipped gear. The gear bodies are rigid but the contact surfaces between the gears are modeled as deformable flex-bodies. The nonlinear contact force, $F = K(d)^e$ — cv, is composed of an elastic and damping portion [16], d is the penetration depth. The damping force, *cv*, is proportional to impact velocity, *v*. The stiffness coefficient, *K*, is taken to be the average value of stiffness over one tooth mesh cycle. The force exponent, e, was determined from trial simulations. The damping coefficient generally takes a numeric value between 0.1% - 1% of *K*. The determination of force exponents however is not obvious and must be based on experience.

The MSC.ADAMS IMPACT algorithm was chosen as the contact force model because of its robustness in numerical integration. The restitution model is extremely sensitive to the duration of the contact event, and is best suited for impulse type simulations. It is not ideal for time histories that include a large number of contact events in which the force vector is not known beforehand. The stiffness parameter is reasonable for this lightly loaded steel gear pair, and was determined via a trial and error method. The response of interest occurs over a very short time interval, around one hundred milliseconds. Because the damping force in meshing gears is such a small percentage of *K*, its affect on the simulation results is not significant. Therefore, the damping coefficient is kept as near to zero as possible to simplify the numerical solver routine. Penetration depth is defined here as the depth at which the damping force becomes active. Similarly, modification of this value does not have a significant effect on response of either gear. The geometric gear pair parameters and MSC.ADAMS contact parameters are shown in Table 1.

The eccentric tooth is generated by rotating the involute profile along the base circle of the pinion by a very small, arbitrary angle that does not cause mesh interference. Similarly, the chipped gear is created by removing a reasonable amount of mass from a single tooth. From the defined gear backlash, the center distance of the gear pair is calculated as 2.705 in [18].

2.2 Simulation results and discussions

Combined with gear profile errors, backlash may cause loss of contact between gear teeth. This may induce consecutive single-sided and/or double-sided impacts and generate large impact forces and large vibration. R_p and R_g are the radii of the base circles of pinion and gear, respectively. The relative displacement between the two mating teeth profiles along the line of action is represented as, $S = R_g\theta_g - R_p\theta_p$. Obviously, when S in bigger than the gear backlash B, there is contact between pinion and gear. For a simple spur set this equation should be true at all times, $-B \leq R_g\theta_g - R_p\theta_p \leq$ B.

Fig.3 shows relative displacement S along the line of action with pinion initial velocity ω_{input} = 100 rad/s for a perfect meshing pair and for a pair with eccentric tooth on the pinion. It is interesting to notice that the back collision takes place

during the separation of the gears. Successive double-sided impacts are observed on the alternating surfaces of the meshing pair. The early motion of Fig.3 is outside ± *B* because of the penetration required by the impact force algorithm. As time increases, penetration decreases and the period between impacts increase for both perfect gear and eccentric gear pairs.

Furthermore, since each point on this plot determines a precise orientation of the mating teeth of each gear, the geometric condition of the eccentric pinion tooth causes an interesting result. More "oscillations" have occurred in the same amount of time. This can be explained by considering that the tooth itself is larger, and therefore it has less space to move within the backlash band of *2B*. Upon startup the eccentric tooth will contact with the mating tooth earlier than it would with perfect geometry.

Fig.4 illustrates the angular velocity of the gear for both a perfect gear pair and a chipped gear pair with a pinion initial velocity and constant applied torques. As contact with the gear occurs, the pinion and gear velocities both change rapidly.

These large magnitudes, which occur for the first 20 ms, are due to the pinion's initial velocity. This transient response dies out quickly, and only the effects of the constant applied torques are observed. Both pinion and gear experience single-sided impacts, shown in Fig.4.

The effect on the number of impacts is the opposite of that seen with the eccentric tooth presented in Fig.3. It takes a little longer for the pinion to contact the gear because the gear's involute profile has been modified. Close inspection shows that the chipped gear case has less direction changes than the perfect case, and hence less impact events. This is a clear representation of double-sided impacts.

3. Crank-Slider Mechanism with Two-stage Gear Train

3.1. Multi-body kinematic model of crank-slider mechanism with two-stage gear train

In order to investigate how the interaction of backlash and manufacturing errors affects the dynamic behaviors and contact forces of a more complicated gearing system, a crank-slider mechanism with two-stage gear train is studied. The gear design parameters and simulation parameters are shown in Table 3 and Table 4, respectively. Fig.5 and Fig.6 show the two-stage gear train and crank-slider mechanism respectively.

3.2 Free Vibration Simulation Results and Discussion

The “perfect" waveform represented in Fig.7 is the response of all four gears with perfect geometry and prescribed backlash. The "chipped" curve is the response of an input pinion with a chipped tooth, all other gears are perfect. The coordinate orientation is such that a force *from the pinion to the gear* is considered positive. This simulation emulates the machine operating at steady-state conditions and suddenly losing power. The system is given an initial velocity on each shaft that corresponds to its rotary speed under operating conditions.

From the top two plots of Fig.7, the initial position of the gears is such that neither stage is in contact at the beginning of the simulation. Therefore, all three shafts are rotating without any impacts until Gear C touches Gear D at approximately 12 ms. Gear B touches Gear A around 15 ms, causing the contacts in Stage 1 to inrease in frequency for the next 20 ms. The response of the intermediate shaft is due to a superposition of the impact in Stage 1 and Stage 2. The angular velocity of the intermediate shaft is shown to be combination of the other two shafts' angular velocities.

Double-sided impacts are clearly evident in the Y-Component of Force in Stage 1. For the chipped pinion case the impact force occurs at an earlier time. This can be explained in part through the reduction in intertia. The mass moment of interia of the perfect input pinion is Izz = 1.06e-3 kg-m^2, while the chipped tooth pinion is I_{zz} = 1.04e-3 kg-m^2. This is a reduction of 1.76%. The chipped pinion will experience a larger acceleration for a given impact force. The teeth neighboring the chipped tooth will contact the mating gear sooner than it would with the standard inertia.

The force response in Stage 2 is depicted in Fig.8. The first and second contacts occur at nearly the same time for both the perfect and chipped cases. With perfect mesh geometry, Gear D experiences three single-sided impacts for $10 \leq t \leq 30$ ms. With a chipped pinion tooth, Gear D only experiences two single-sided impacts during the same interval.

An impact occurs in Stage 2 before Stage 1, at first this may seem counter-intuitive. The initial velocities given to each shaft are based upon their rated operating speed. The bearings are modeled as frictionless, constraining all degrees of freedom except for rotation in the normal plane. The relative velocity on the pitch circle of Gear C and Gear D is slightly larger than

between Gear A and Gear B. For intial conditions in which the relative velocity between Gear A and Gear B is larger than between Gear C and Gear D, the opposite would occur.

The system is modeled as the interaction of three rigid bodies. The first is the input shaft and Gear A. The second is Gear B, the Intermediate Shaft, and Gear C. The third is Gear D, the Output Shaft, and the Crank. The third body has an intertial mass at least one order of magnitude larger than the other two bodies. Its velocity changes more slowly than for the other two bodies. due to intertia effects. The small delay between responses around 18.5 ms can be attributed to the chipped tooth. Because the tooth is missing the force response in Stage 2 is slightly delayed.

Fig.9 shows the relative displacment between Gear C and Gear D in Stage 2. Any point on this plot defines the position for both Gear C and Gear D for any give time. The contacts in the first stage directly effect the position of Gear C. Due to the interaction of Gear A and Gear B, Gear C oscillates back and forth as it moves between teeth of Gear D. The quantity $S = R_g\theta_g - R_p\theta_p$ for the second stage appears as a jagged line. These small peaks correspond directly to the Force in Stage 1, shown previously in Fig.8. Once Gear C makes contact with Gear D the response becomes smoother. The effect is still there, but the speed of Gear D is now changing more rapidly and these smaller position changes are more difficult to distinguish. For the case with a chipped tooth on the input pinion, the entire curve is shifted forward in time. Although the impacts in Stage 1 occur earlier, the overall effect in Stage 2 is delayed. The missing tooth causes Stage 1 to become more excited, as a result it takes longer for the contact in Stage 2 to occur.

3.3 Forced Vibration Simulation Results and Discussions

A step torque of the form $T(1 - et\sim)$ is applied to the input shaft with amplitude of 149.123 N-m at 100 ms. to simulate an accelerating condition.

From Fig. 10, the gears in each mesh come to an equilibrium position in which they remain in contact. This must be true for the system to be transmitting power. The driving teeth approach the "surface" of the driven teeth, oscillating with less amplitude as time increases. The decrease in oscillation amplitude is most notable in Stage 1. The quantity $S = Rg\theta g - Rp\theta p$ waveforms approach the "surfaces" indicated.

From Fig. 11, the impacts in both stages increase in magnitude with time, and also occur at increasingly shorter intervals. The force in Stage 2 is larger because Gear D is being driven, effectively by the torque on the Input Shaft. The large inertia of this third rigid body must be overcome solely with the force from Gear C to Gear D in Stage 2. The Stage 2 impacts carry the energy accumulated in the Stage 1, and therefore have a larger amplitude.

4. Conclusions

A non-linear multi-body dynamic software model has been developed for a fixed-axis transmission and a crank-slider mechanism to demonstrate the effects of dynamic loading on gear teeth. The stiffness, force exponent, damping, and friction coefficients for the MSC.IMPACT force algorithm are derived for a practical transmission. Single-sided impacts are observed in a spur pair when the pinion is given an initial velocity, and torques of equal magnitude but opposite direction are applied to each gear. The dynamic behavior of the intermediate shaft of a two stage crank-slider mechanism is shown to be a superposition of the impact forces acting in each mesh. The geometric error of a chipped tooth on the pinion gear of this mechanism causes a delay in the contact forces in the second stage. A realistic driving step torque creates impact forces which increase in both magnitude and frequency as the crank accelerates to its operating speed.

5. Acknowledgement

The authors acknowledge the Donald E. Bently Center for Engineering Innovation at California Polytechnic State University San Luis Obispo for support of this work.

REFERENCES

1. Dubowsky, S. and Freudenstein, F., "Dynamic Analysis of Mechanical Systems With Clearances, Part 1: Formulation of Dynamic Model", *ASME Journal of Engineering for Industry*, Vol. 93, Feb. 1971, pp. 305-309.

2. Dubowsky, S. and Freudenstein, F., "Dynamic Analysis of Mechanical Systems With Clearances, Part 2: Dynamic Response", *ASME Journal of Engineering for Industry*, Vol. 93, Feb. 1971, pp. 310-316.

3. Azar, R. C., and Crossley, F. R. E., "Digital Simulation of Impact Phenomenon in Sour Gear Systems", *ASME Journal of Engineering for Industry*, Vol. 99, Aug. 1977, pp. 792-798.

4. Yang D.C.H. and Sun Z.S., "A Rotary Model for Spur Gear Dynamics", Transactions of the ASME, *Journal of Mechanisms, Transmissions and Automation in Design*, Vol. 107, Dec. 1985, pp. 529-535.

5. Özgüven H.N. and Houser D.R., "Mathematical Models used in Gear Dynamics – A Review", *Journal of Sound and Vibration*, 121(3), 1988, pp. 383-411.

6. Parey, A. and Tandon, N., "Spur Gear Dynamic Models Including Defects: A Review", *The Shock and Vibration Digest*, Vol. 35, No. 6, Nov. 2003; pp. 465-478.

7. G. Dalpiaz, A. Rivola and R. Rubini, "Effectiveness and Sensitivity of Vibration Processing Techniques for Local Fault Detection in Gears", *Mechanical Systems and Signal Processing*, Vol. 14(3), 2000, pp. 387-412.

8. Parey, M. El Badaoui, F. Guillet, N. Tandon, "Dynamic modeling of spur gear pair and application of empirical mode decomposition-based statistical analysis for early detection of localized tooth defect", *Journal of Sound and Vibration* Vol. 294, 2006, pp. 547–561.

9. Saeed Ebrahimi and Peter Eberhard, "Rigid-elastic modeling of meshing gear wheels in multi-body systems", *Multi-body System Dynamics* Vol. 16, 2006, pp. 55–67.

10. Tahar Fakhfakh, Fakher Chaari and Mohamed Haddar, "Numerical and experimental analysis of a gear system with teeth defects", *The International Journal of Advanced Manufacturing Technology*, Vol. 25, 2005, pp. 542–550.

11. I. Ciglariˇc and A. Kidriˇc, "Computer-aided derivation of the optimal mathematical models to study gear-pair dynamic by using genetic programming", *Structural and Multidisciplinary Optimization*, Vol 32, 2006, pp. 153–160.

12. M. Pimsarn and K. Kazerounian, "Pseudo-interference stiffness estimation, a highly efficient numerical method for force evaluation in contact problems", *Engineering with Computers*, Vol. 19, 2003, pp. 85–91.

13. Meagher, J., Wu, X., Kong, D., Lee, C, "A Comparison of Gear Mesh Stiffness Modeling Strategies", *IMAC XXVIII a Conference on Structural Dynamics*, Society for Experimental Mechanics, Jacksonville, Florida USA, February 1 –4, 2010.

14. Ebrahimi S. and Eberhard P., "Rigid-elastic modeling of meshing gear wheels in multi-body systems", *Multi-body System Dynamics*, Vol. 16, 2006, pp. 55–71.

15. Kong, D., Meagher, J., Xu, C., Wu, X., Wu, Y., "Nonlinear Contact Analysis of Gear Teeth for Malfunction Diagnostics", *IMAC XXVI a Conference on Structural Dynamics*, Society for Experimental Mechanics, Orlando, Florida USA, February 4 –7, 2008.

16. MSC Inc., *MSC ADAMS reference manual*.

17. Machinery's Handbook 28th Larger Print Edition.

18. Raymond J. Drago, Fundamentals of Gear Design, 1988.

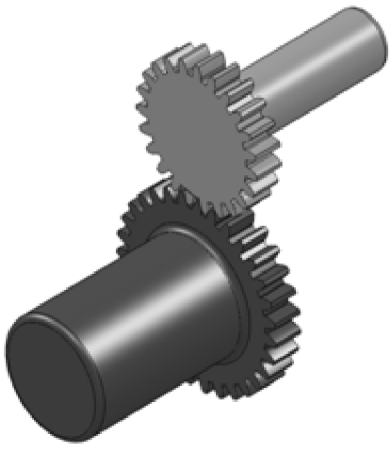

Fig.1 A pair of meshing gears

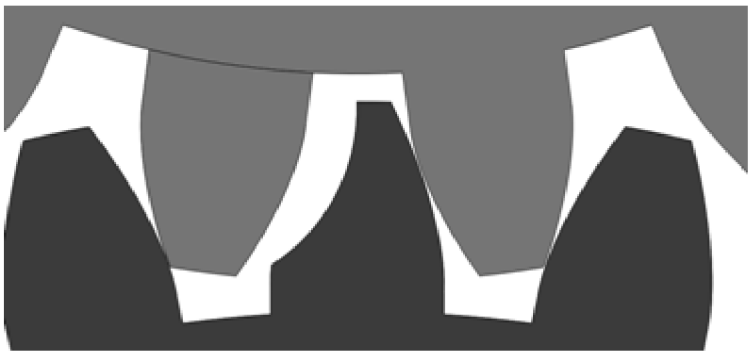

Fig.2 Eccentric pinion tooth with chipped gear

Table 1. Geometric Parameters and Simulation Contact Force.

Algorithm		MSC.ADAMS IMPACT
Stiffness		2e7 [lb_f/in]
Force Exponent		2.2
Damping		2e-2 [% stiffness]
Penetration		1e-7 [in]
Diametral Pitch	P_d	10 [teeth/in]
Pressure Angle	Φ	20 [deg]
Face Width	F	0.5 [in]
Pinion	p	23 [teeth]
Gear	g	31 [teeth]
Backlash	*B*	0.004 [in]

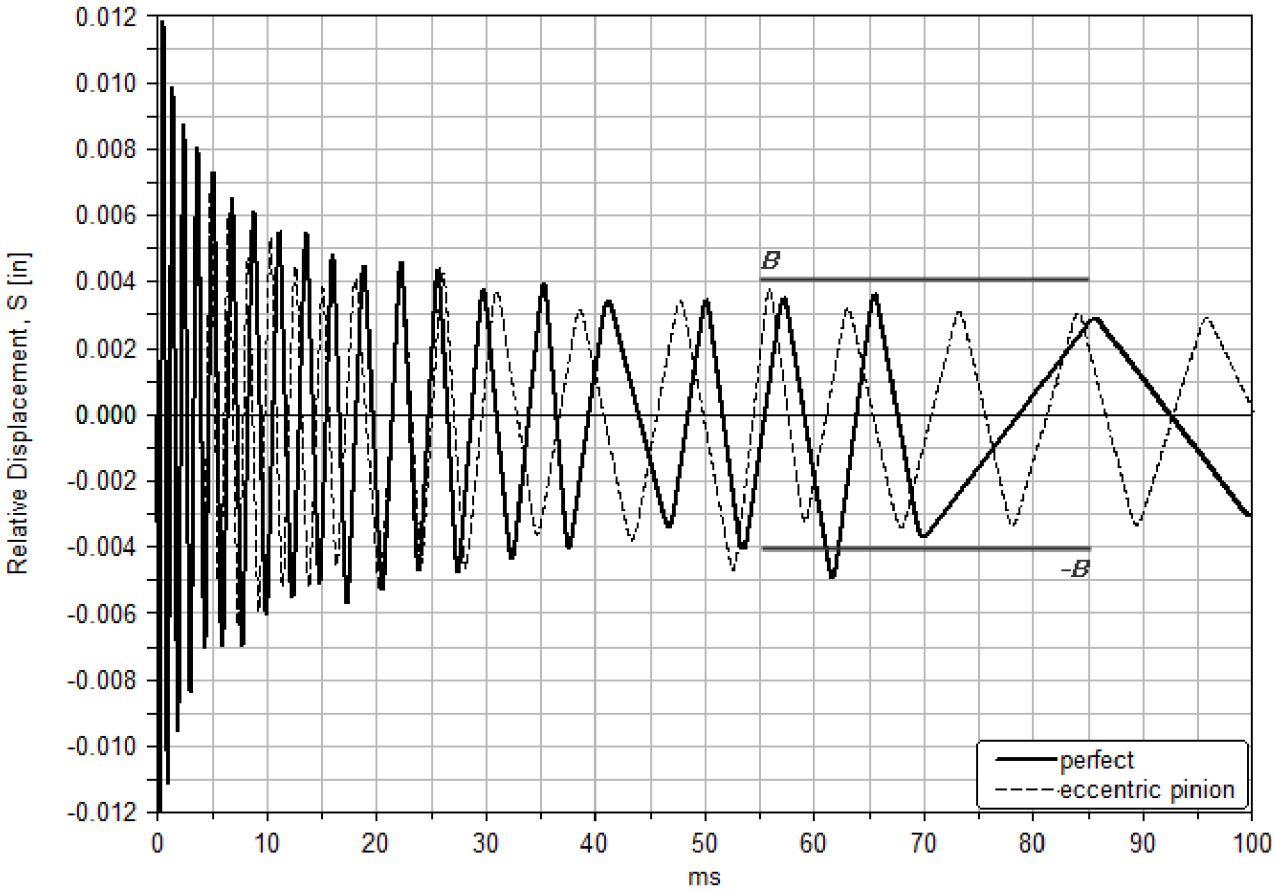

Fig.3 Relative displacement S along the line of action with pinion initial velocity ω_{input} = 100 rad/s

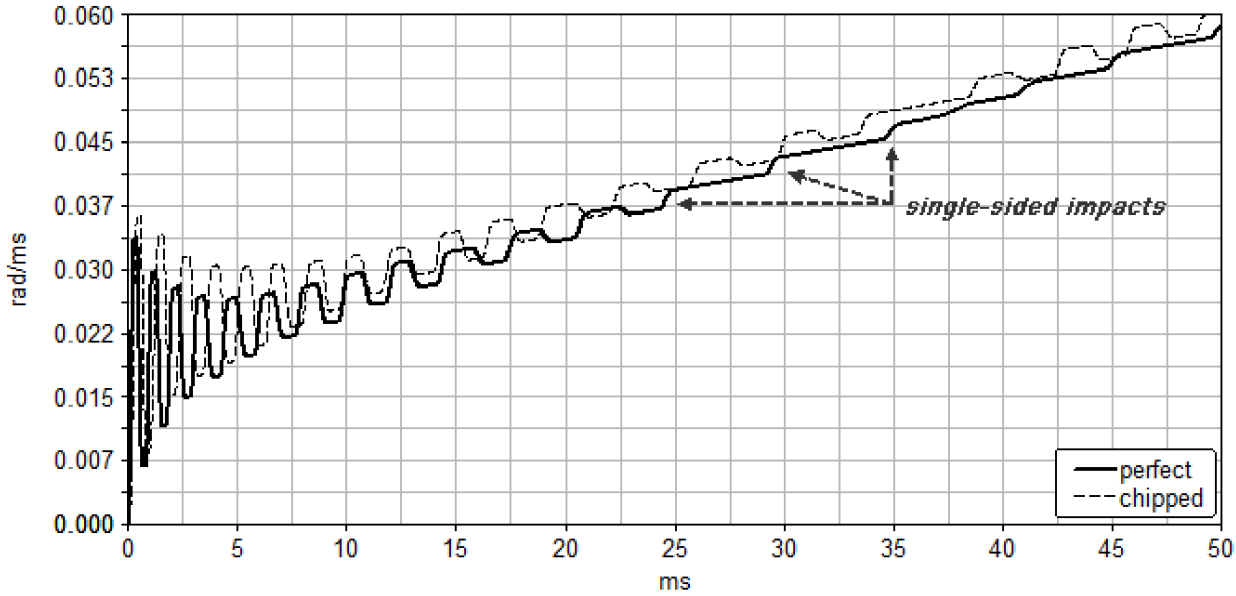

Fig.4 Angular velocity of the pinion with initial velocity 100 rad/s; 3 lbf-in torque applied to pinion; -3 lbf-in torque applied to gear.

Table 3. Gear Design parameters

Modules m [mm/tooth]	m_1=4; m_2=5
Number of teeth	Z_a=17; Z_b =60; Z_c=19; Z_d =72
Standard Pitch circle diameter *d*(mm)	d_a=68; d_b = 240; d_c=95; d_d =360
Total gear ratio	13.375
Pressure angle	20°

Table 4. Simulation parameters

Backlashes [mm]	B_1 = 0.05; B_2 = 0.08
Material properties	E = 2.07 x 10^{11} Pa; ν = 0.29; ρ = 7801 kg/m^3
Force exponent	2.2
Penetration	10^{-7} mm
Stiffness	2 x 10^7 N/mm

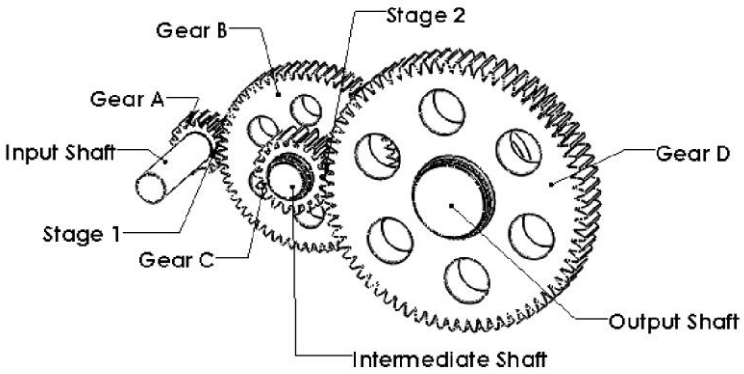

Fig.5 Two-stage gear train

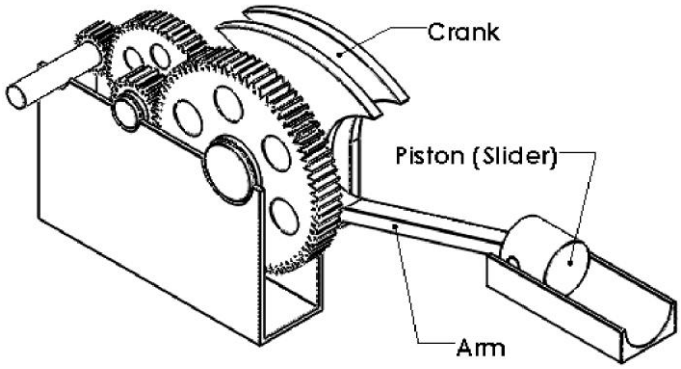

Fig.6 Crank-Slider Mechanism

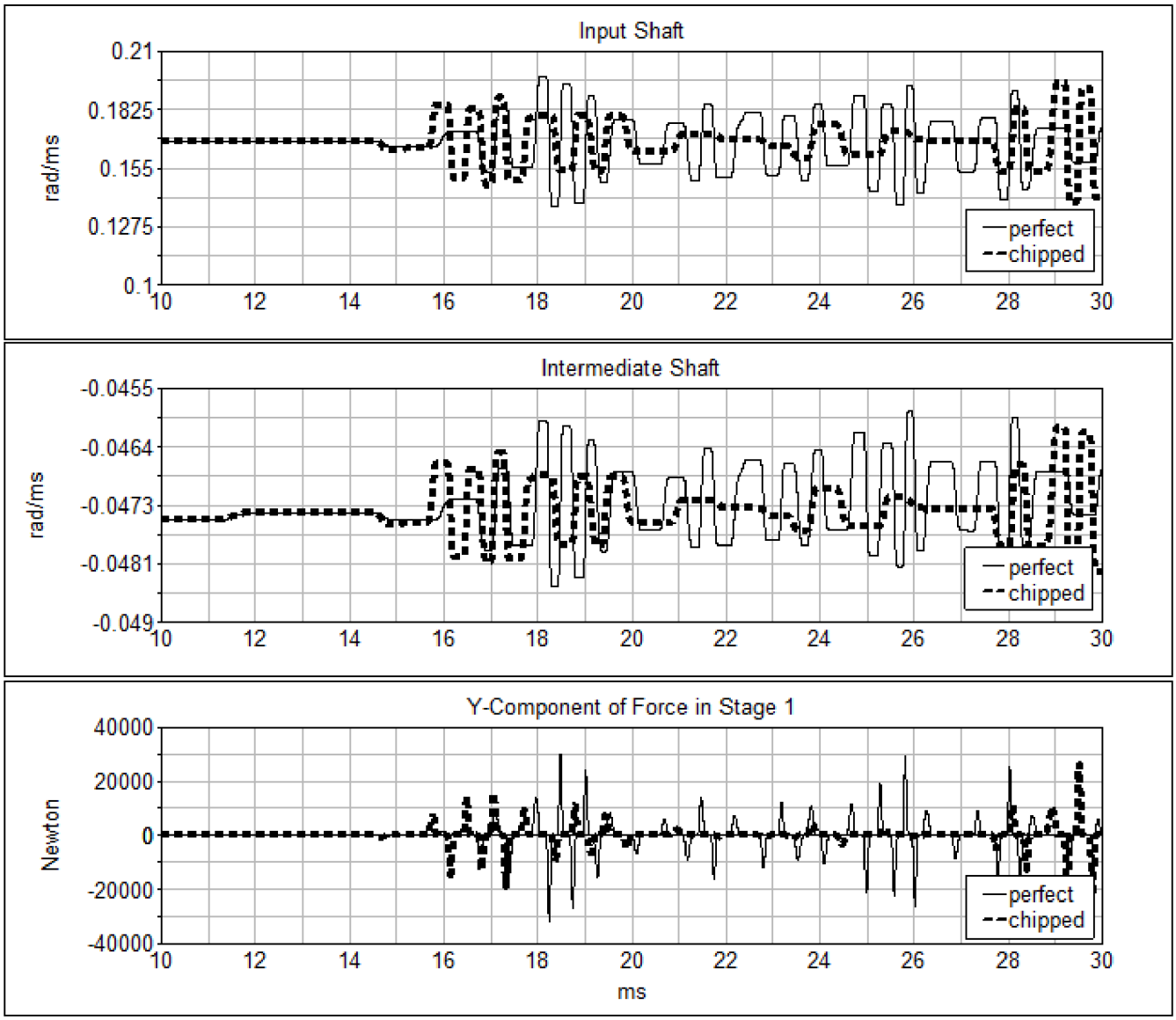

Fig.7 Free vibration response with input shaft, 167.5 rad/s; intermediate shaft, -73.5 rad/s; output shaft, 12.5 rad/s.

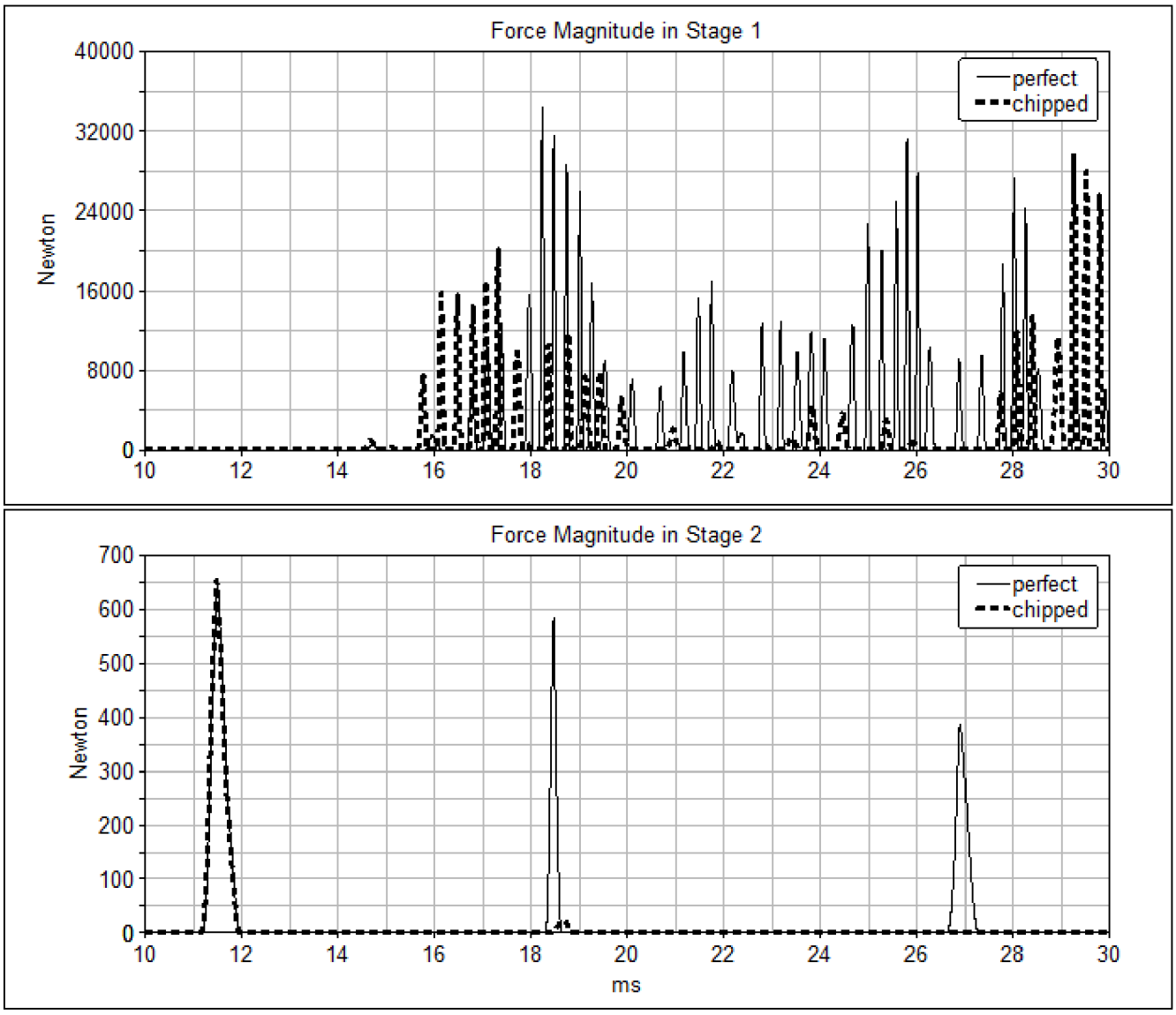

Fig.8 Comparison of the force magnitudes of Stage 1 and Stage 2 with the initial conditions: input shaft, 167.5 rad/s; intermediate shaft, -73.5 rad/s; output shaft, 12.5 rad/s.

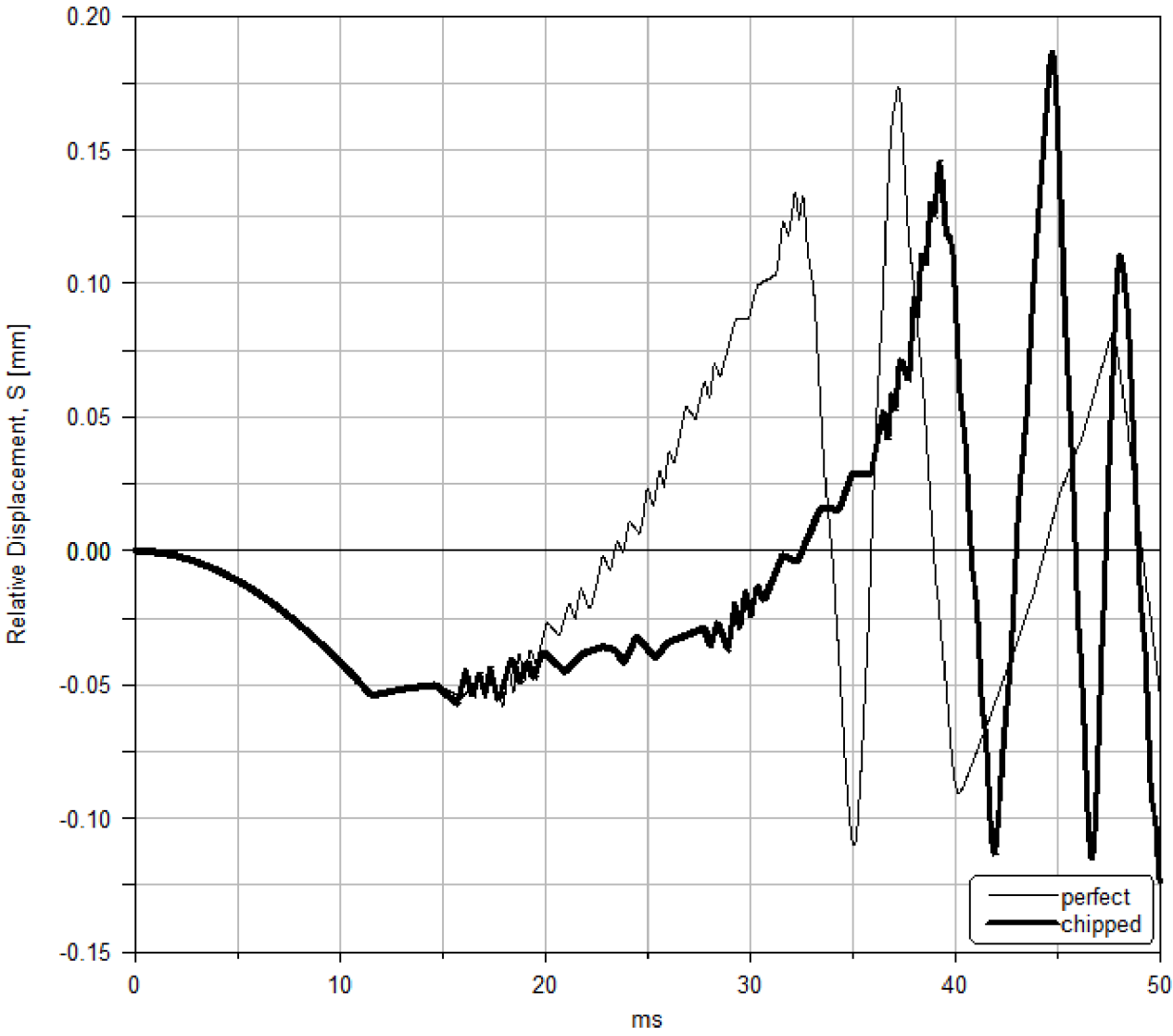

Fig.9 Relative displacement S along the line of action on stage 2 with the initial conditions: input shaft, 167.5 rad/s; intermediate shaft, -73.5 rad/s; output shaft, 12.5 rad/s.

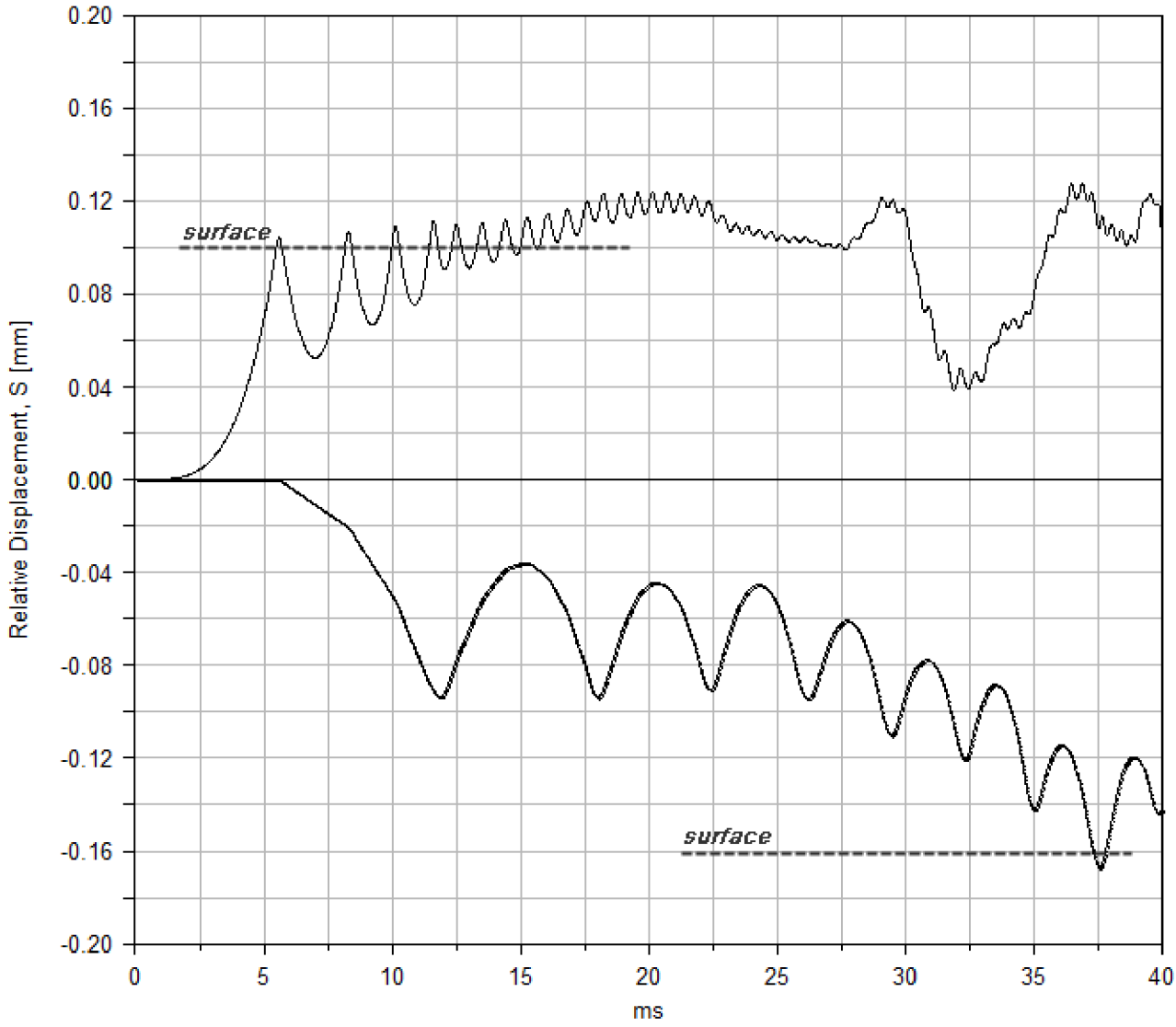

Fig.10 Comparison of relative displacements S along the line of action on stage 1 and stage 2 with step input torque 149.123 N-m

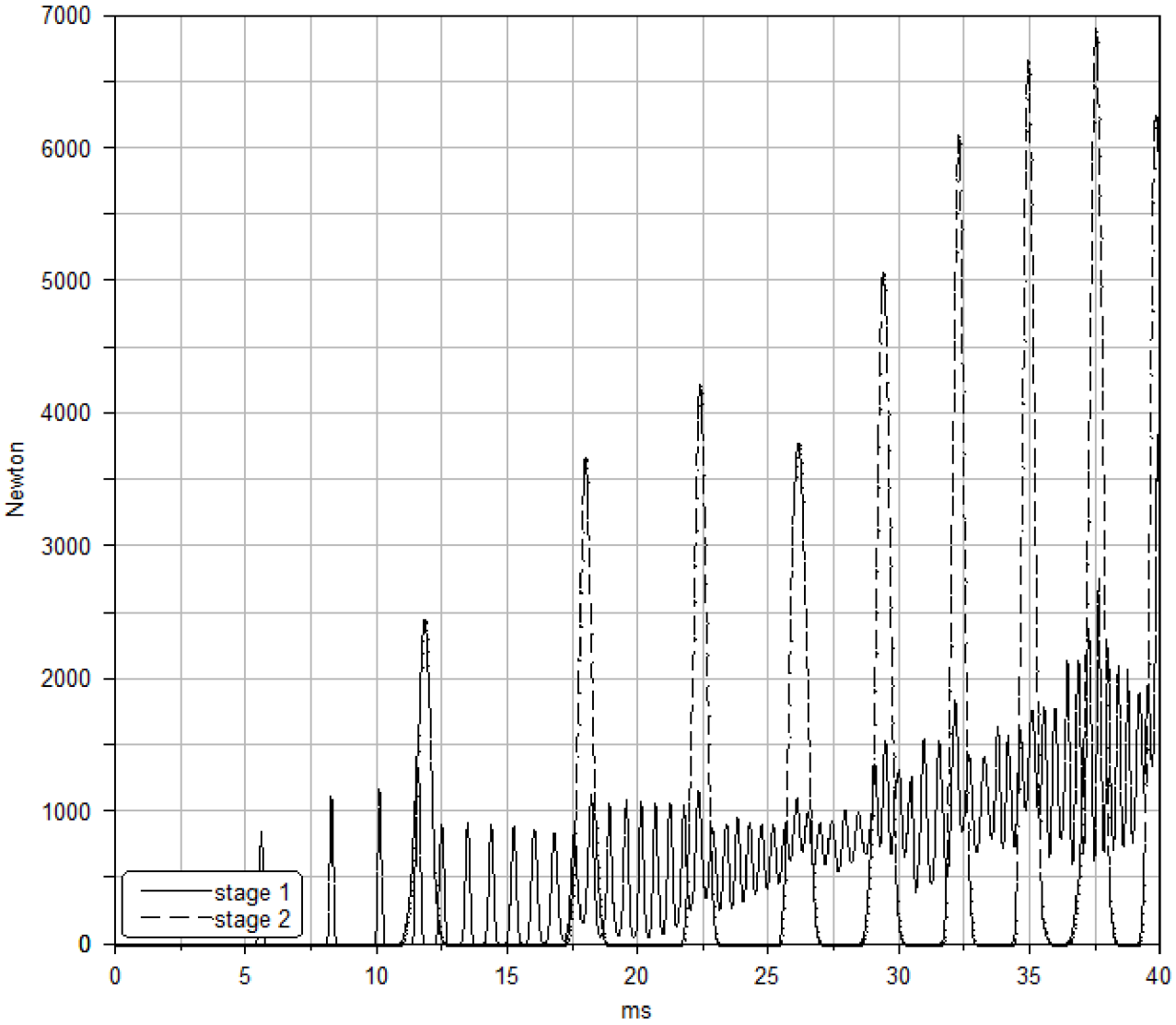

Fig.11 Comparison of the force magnitudes on stage 1 and stage 2 with step input torque 149.123 N-m